

## Bismuth-modified Hydroxyapatite Carbon Electrode for Simultaneous *in-situ* Cadmium and Lead Analysis

Aamir A. A. Khan, Mohd Azmuddin Abdullah\*

Department of Chemical Engineering, Universiti Teknologi PETRONAS, Bandar Seri Iskandar, 31750, Tronoh, Perak, Malaysia

\*E-mail: [azmuddin@petronas.com.my](mailto:azmuddin@petronas.com.my)

*Received:* 5 November 2012 / *Accepted:* 2 December 2012 / *Published:* 1 January 2013

---

Modification of carbon electrode with hydroxyapatite (HA) and Bismuth (II) was carried out to enhance Cd<sup>2+</sup> and Pb<sup>2+</sup> deposition through HA ion-exchange. The interacting ability of the Bi film and HA on the electrode surface was evaluated for simultaneous determination of Cd<sup>2+</sup> and Pb<sup>2+</sup> using cyclic and square wave anodic stripping voltammetry, at deposition potential of -1.0 V in 0.1M acetate buffer for 240 sec, followed by square wave potential scan from -1.0 V to -0.2V. Stripping voltammogram showed current peaks corresponding to Cd<sup>2+</sup> and Pb<sup>2+</sup> limit of detection (LOD) of 5 µg/l and consistent up to 150 µg/l. Sensitivity and selectivity of the modified electrodes for Cd<sup>2+</sup> and Pb<sup>2+</sup> were also determined.

---

**Keywords:** Electrochemical Sensor, Carbon electrodes, Environmental Monitoring, Hydroxyapatite, Bismuth

### 1. INTRODUCTION

Human activities are the major contributing factors that lead to environmental imbalance we are witnessing today. Heavy metals are naturally present in igneous rocks and metallic minerals, but become major pollutants as a result of industrial and mining activities, use of fertilizers and pesticides during agricultural processes, mining activities, and release from fuels and microelectronic products [1]. Anodic stripping voltammetry (ASV) is recognized as a powerful electroanalytical methodology in the trace metal analysis. The advantages are heavy metal determination of picomolar level can be achieved with high sensitivity, capability for several real-time metal analytes application, relatively low cost of instrumentation, and readily portable and miniaturized. ASV mostly involves pre-concentration of the analyte on the hanging mercury drop or mercury film electrode [2]. Attempts have been made to develop mercury-free electrodes as mercury toxicity is a major concern [3-7].

Bismuth (Bi) is an environmentally-friendly element, with low toxicity, and has widespread pharmaceutical use [8-10]. Bismuth film electrodes (BiFEs) are promising sensors, exhibiting analytical properties similar to Hg film electrodes and thus gain wide interest in the field of electrochemical analysis [5, 8]. BiFEs are prepared by plating a thin bismuth film on an appropriate substrate material. Bi deposition step involves solid metal analyte deposit on the surface of Bi film electrode. Heavy metal analyte film is uniform with respect to the energy required for the anodic stripping process. The analytical properties of BiFEs in voltammetric analysis, are attributed to the property of bismuth to form “fused alloys” with numerous heavy metals, analogous to the amalgams that mercury forms [8]. Both *in situ* or *ex situ* bismuth film and bulk bismuth electrodes provide excellent stripping response, and the uniform metal analyte film is due to this unique ability of Bi to form fused multi-component alloys with heavy metals [5, 8, 11-15].

Hydroxyapatite (HA) consists of mainly calcium phosphate, having sorption capacity for divalent heavy metal ions. Due to its similarity with human bone structure, HA crystals have been coated on copper using electrochemical method leading to its potential application as biocompatible and bioreactive substrates [16]. Heavy metal ions interact with HA modified electrode by preconcentration with surface complexation, followed by simultaneous adsorption on HA, and calcium ion substitution coupled with diffusion on the electrode surface. It shows increased detection limits for  $\text{Cd}^{2+}$  and  $\text{Pb}^{2+}$  resulting in higher sensitivity as compared to traditional electrode.

The objectives of the study were to develop robust, mobile and user-friendly electrochemical detection methods for  $\text{Cd}^{2+}$  and  $\text{Pb}^{2+}$  based on Bismuth-modified hydroxyapatite carbon electrodes. Special emphasis was given on the selectivity and sensitivity of detection. The parameters optimized include the deposition time, electrolyte type and pH, potential and concentration of modifier.

## 2. METHODOLOGY

Stock solution of  $\text{Cd}^{2+}$  and  $\text{Pb}^{2+}$  of 1000 ppm were obtained from Merck. All solutions were prepared by ultrapure deionized water (Elga Purelab Ultra). Supporting electrolytes and metal solutions of lower concentrations were prepared fresh before experiments. Graphite powder and paraffin oil were used for carbon electrode preparation. Hydroxyapatite was obtained from Sigma-Aldrich. Bismuth nitrate was supplied from Merck. All the chemicals used were of analytical grade.

The carbon paste electrode (CPE) was prepared by mixing graphite powder with paraffin in an agate mortar, ground, and later packed into a cavity (3mm internal diameter) of a Teflon tube. Redundant paste was mechanically removed. Copper wire was connected to the paste via the inner hole of the tube to provide electrical contact. HA carbon modified electrode (HA-CME) was prepared by adding different content ratio of HA:graphite from 1:5 to 1:20. CME preparations were carried out at room temperature.

Cell for electrochemical measurements comprised of AgCl/KCl (Metrohm) reference electrode, graphite bar as auxiliary electrode and the modified carbon working electrode. Electrochemical measurements were carried out by  $\mu\text{Stat}400$  bipotentiostat/galvanostat, battery-powered, supplied by DropSens, (Spain). It was connected to a computer and controlled by *dropview* software. SWASV was

applied for electrochemical measurements using square-wave potential ramp with a frequency of 25 Hz, a potential step of 5mV, and an amplitude of 50 mV. The electrochemical accumulation step was usually at  $-1V$  for 240 sec, an equilibration period of 30 sec, followed by a square-wave voltammetric stripping scan from  $-1.0$  to  $-0.2$  V. Electrolyte solution was added to the electrochemical cell, followed by addition of lower concentration of  $Cd^{2+}$  and  $Pb^{2+}$  ( $0-200 \mu\text{g/l}$ ) with pH adjusted to pH 7.6.

*In-situ* Bismuth was applied by preparing 100ppm stock solution of  $Bi^{2+}$  and added to the sample cell containing the analyte. Fixed potential of  $-1.0$  V was applied for electrochemical film deposition, along with analyte deposition for 240 sec, an equilibration period of 30 sec, followed by electrochemical stripping potential.

To eliminate matrix effects, standard addition method was used. Calibration curves were developed and linear regression and detection limits were calculated. All data were obtained at room temperature ( $\sim 25$  °C). Standardization for analyzing heavy metal ions in trace quantities was employed using Atomic Absorption Spectrometer (AAS, Hitachi Z-5000) using graphite furnace. To validate the developed method for environmental applications, lead and cadmium ions in the spiked lake water samples were determined. Samples were collected from two different lakes in Universiti Teknologi Petronas, filtered through filter paper (Whatman No. 1, England) to remove suspended particles, and filtrate adjusted to pH 8 for analysis.

### 3. RESULTS & DISCUSSION

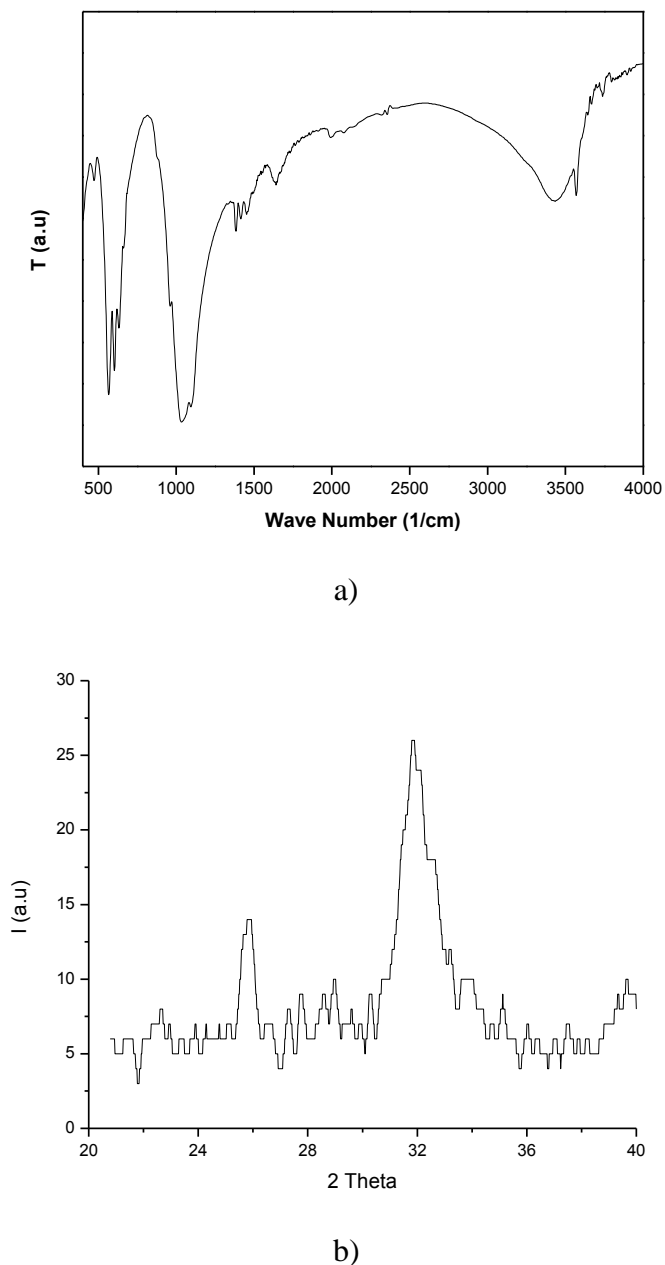
#### 3.1. Characterization of HA and CME

Figure 1a shows the FTIR spectrum for chemical functional groups present in synthesized HA. Peaks at  $3600$  to  $3300 \text{ cm}^{-1}$  suggest hydroxide stretching [17] and peaks between  $1457$  to  $1384 \text{ cm}^{-1}$  and  $1638 \text{ cm}^{-1}$  correspond to the carbonate ions [18]. The band at  $873 \text{ cm}^{-1}$  could be assigned to the  $HPO_4^{2-}$  group [18, 19], whilst the weak intensity bands between  $2200$  and  $1990 \text{ cm}^{-1}$ , and  $1032$  and  $472 \text{ cm}^{-1}$  correspond to  $PO_4^{3-}$  [19, 20]. The IR peak appearing at  $602 \text{ cm}^{-1}$  is assigned to the vibrations of OH for the adsorbed water molecules [21]. The XRD diffractogram (Figure 1b) of synthesized HA exhibits broad diffraction peaks indicating low crystallinity with mesoporous structure (JCPDS 9-432). This may allow for greater interaction, sorption and ion exchange of analytes with the sensing material.

The SEM and FESEM images (Figure 2) show that HA comprises of small meso-porous particles with mean particle sizes of  $150 \pm 50$  nm in length, similar to that reported earlier [22, 23]. EDX spectra clearly show distinct peaks of P and Ca elements. The HA-CME surface presents disorderly HA distribution in between the graphite flakes, suggesting that addition of HA provides extra surface area for sorption of metal ions which could enhance the current response, and therefore the sensitivity.

The efficacy of HA-CME was evaluated by cyclic voltammetry, recorded for 5mM potassium ferricyanide in 0.1M KCl at 100 mV/sec scan rate. Increase in scan rate has resulted in an increase in electron transfer as evident in the peak value difference between anodic and cathodic potential. In order to evaluate the electron transfer at the surface of modified electrode and the surface areas,

100mV/sec scan rate was selected due to faster electron transfer. CV was recorded using 5.0 mM  $K_3Fe(CN)_6$  as test analyte in 0.1M KCl at 100 mV/sec scan rate for CPE, HA-CME, CPE with Bi(II) and HA-CME with Bi(II) (Figure 3).



**Figure 1.** a) FTIR spectrum, b) XRD diffractogram of synthesized HA

The difference in electron transfer between CPE and HA-CME can be clearly distinguished, with higher redox peaks in HA-CME with Bi(II) indicative of the presence of HA and Bi(II) on the surface. HA provides sorption at electrode surface [24] and  $Ca^{2+}$  increases ion exchange capability, whilst Bi(II) forms “fused alloy” with heavy metals which are all important properties for heavy metal analysis [8, 25].

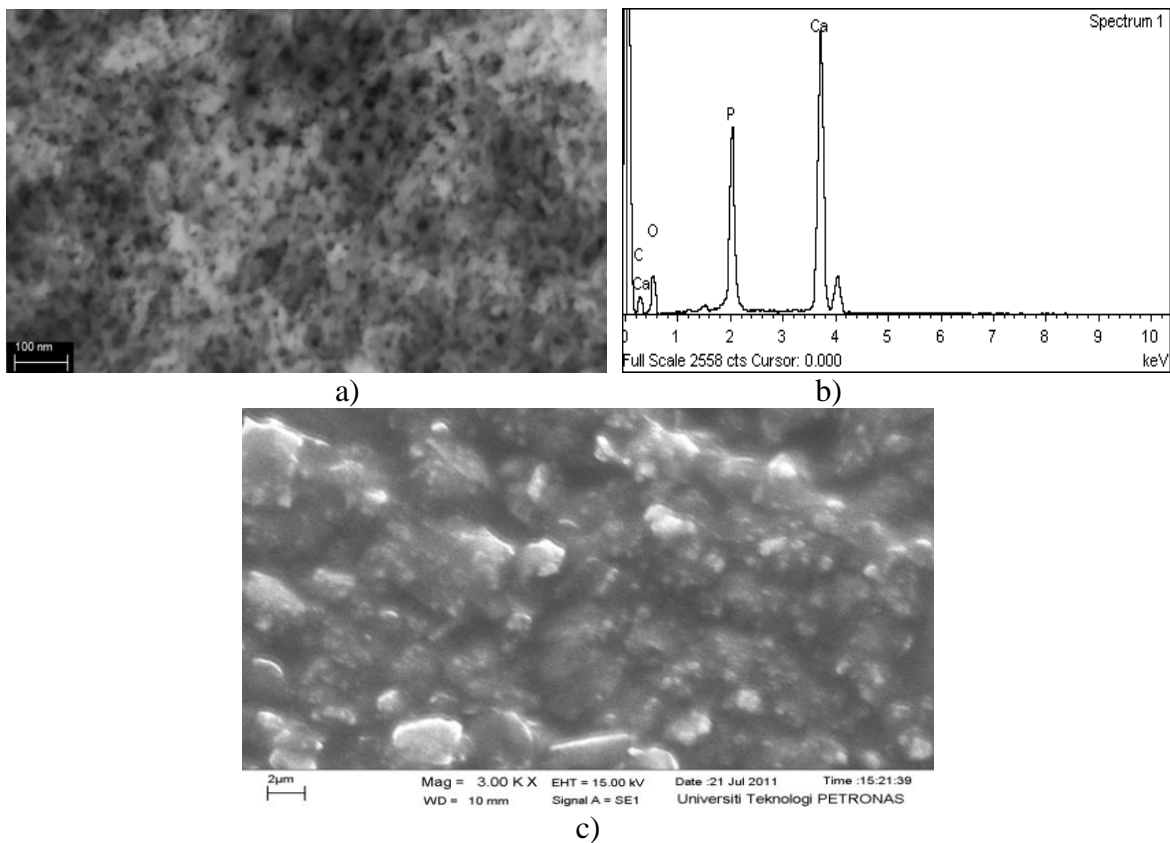


**Figure 2.** a) FESEM image of HA, b) EDX spectra of HA, c) SEM micrograph of HA-CME

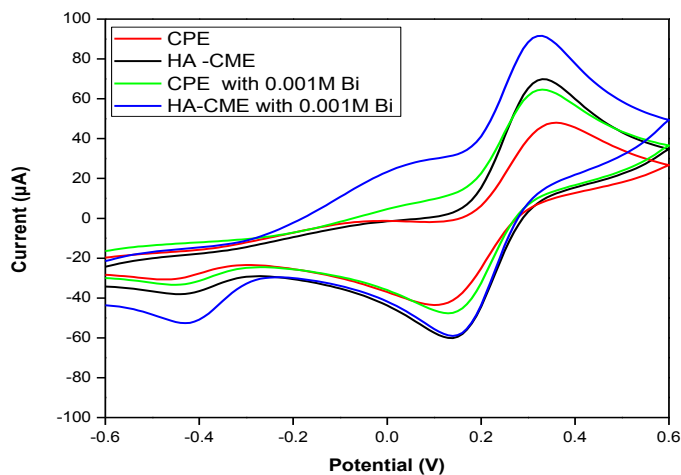
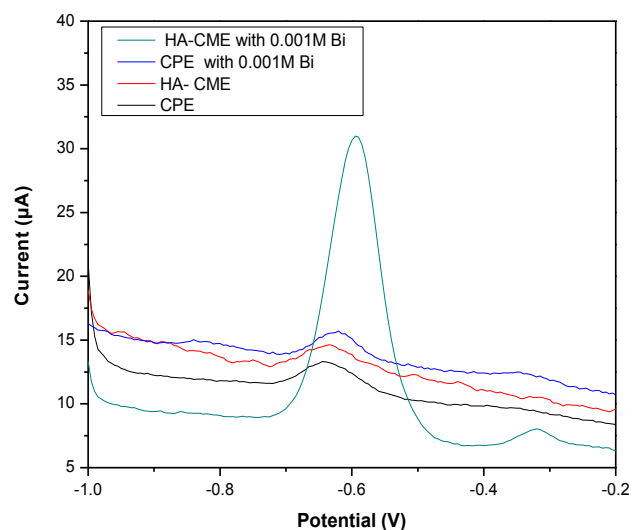


**Figure 3.** Cyclic Voltammogram for 5mM  $\text{Fe}(\text{CN})_6^{-3/-4}$  using CPE, HA-CME, CPE with Bi(II) and HA-CME with Bi(II) in 0.1M KCl and 0.1mV/sec scan rate

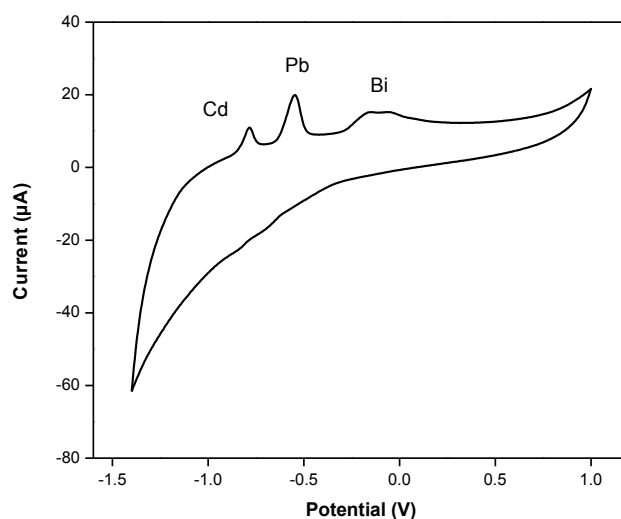
### 3.2. Single $\text{Pb}^{2+}$ and $\text{Cd}^{2+}$ ion detection

SWV analyses for different  $\text{Cd}^{2+}$  and  $\text{Pb}^{2+}$  concentrations were carried out by *in situ* Bi film deposited HA-CME as shown in Figure 4. Clear current peaks for  $\text{Cd}^{2+}$  concentration was observed around -0.8 V, and  $\text{Pb}^{2+}$  at -0.6 V. It was clearly demonstrated that Bi film deposited HA-CME had

attractive electrochemical characteristics, with high sensitivity for both  $\text{Cd}^{2+}$  and  $\text{Pb}^{2+}$ , as compared to HA-CME.



a)



b)

**Figure 4.** a) Stripping voltammogram of different electrodes for 50ppb  $\text{Pb}^{2+}$  in acetate buffer pH 7.6, at 240s deposition time; b) Cyclic voltammogram of Bi film deposited HA-CME 5% for 0.2 ppm  $\text{Pb}^{2+}$  and 0.11 ppm  $\text{Cd}^{2+}$  in acetate buffer pH 7.6, at 240s deposition time

Bi film along with HA offers a good stripping peak having favourable signal-to-background ratio, and relatively free from oxygen interferences during SWV measurements. Calibration for  $\text{Pb}^{2+}$  concentration was carried out with successive additions of 10  $\mu\text{g/l}$  each of  $\text{Cd}^{2+}$  and  $\text{Pb}^{2+}$  in an electrochemical cell of 10 mL under optimized experimental conditions. The peak currents increased linearly with increase of both  $\text{Cd}^{2+}$  and  $\text{Pb}^{2+}$  concentrations in the range 10–200  $\mu\text{g/l}$  (Figs. 5). The

limit of detection (LOD) of  $Pb^{2+}$  was  $5 \mu g/l$ , and for  $Cd^{2+}$  was  $10 \mu g/l$ . The linear regression equation of  $Pb^{2+}$  is given as :- peak current ( $\mu A$ ) =  $4.3308x - 1.4288$ , with a correlation coefficient of 0.984, and for  $Cd^{2+}$  :- peak current ( $\mu A$ ) =  $3.5917x - 2.3548$ , with a correlation coefficient of 0.991.

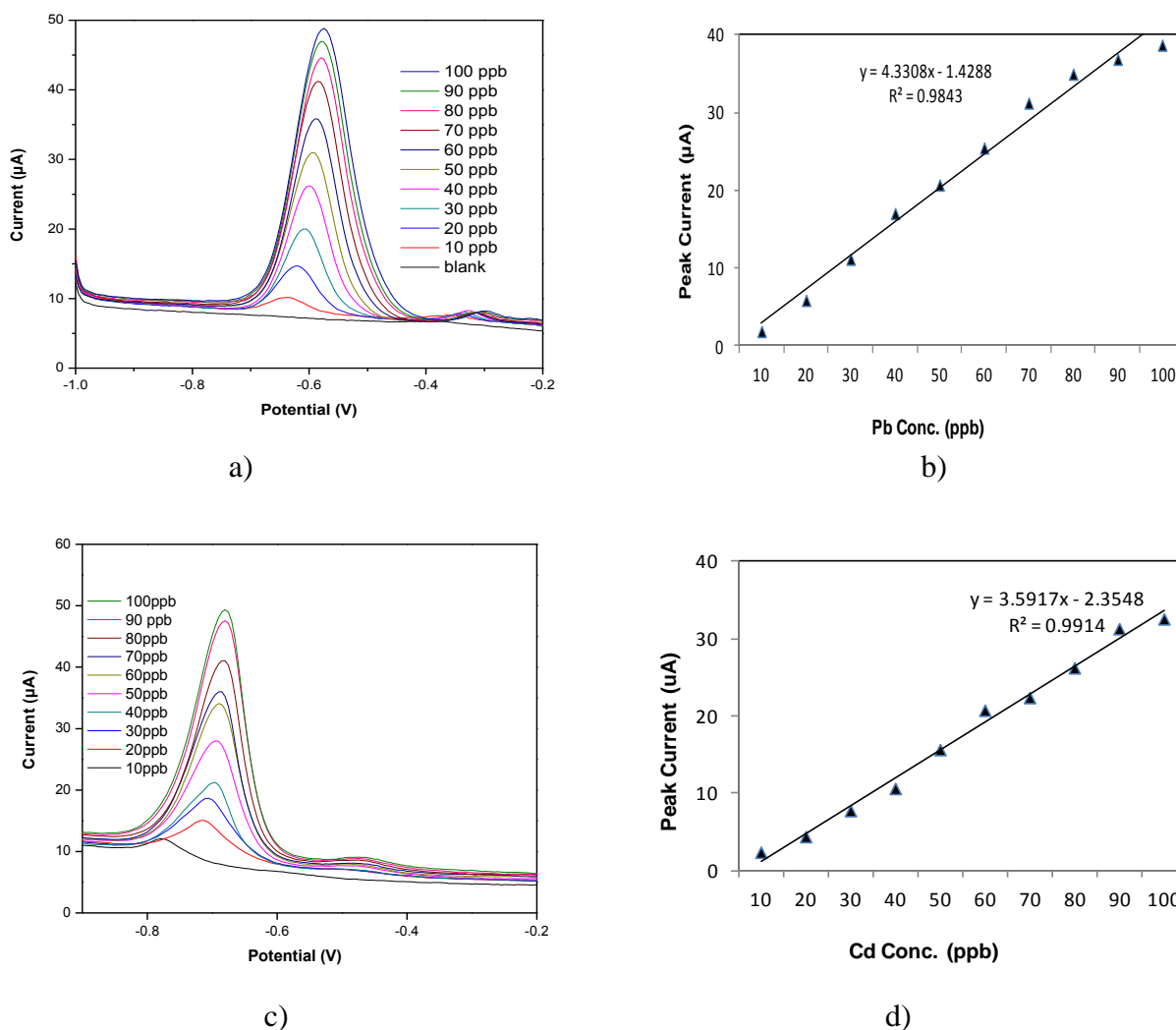


**Figure 5.** a) Stripping voltammogram and b) calibration curve of Bi film deposited HA-CME 5% for different concentrations of  $Pb^{2+}$  in acetate buffer pH 7.6, at 240s deposition time, c) Stripping voltammogram and d) calibration curve of Bi film deposited HA-CME 5% for  $Cd^{2+}$  in acetate buffer pH 7.6, at 240s deposition time.

### 3.3. Multiple $Pb^{2+}$ and $Cd^{2+}$ ion detection

The SWV response at the Bi-HA CME was further studied for simultaneous detection of  $Cd^{2+}$  and  $Pb^{2+}$  (Figure 6). Two well-defined peaks corresponding to  $Cd^{2+}$  at  $-0.8V$  and  $Pb^{2+}$  at  $-0.6V$  can be discerned. The methods were validated by analyzing the lake water spiked sample using the Bi-HA CME and AAS. The results showed good agreement (Table 1) suggesting successful development and implementation of Bi-HA CME for simultaneous lead and cadmium ion detection.

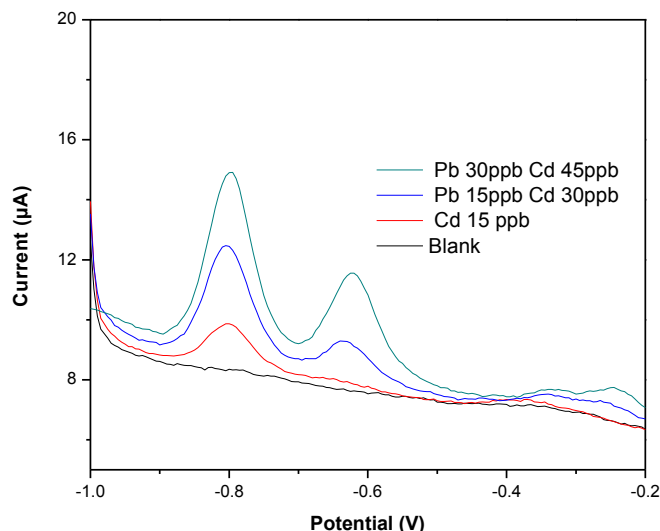


**Figure 6.** Stripping voltammogram of Bi film deposited HA-CME 5% for Cd<sup>2+</sup> and Pb<sup>2+</sup> in acetate buffer pH 7.6, at 240s deposition time

**Table 1.** Determination of lead and cadmium from spiked lake water samples

Sample	Spiked Sample (µg/l)		Bi-HA CME* (µg/l)		AAS* (µg/l)	
	Cd <sup>2+</sup>	Pb <sup>2+</sup>	Cd <sup>2+</sup>	Pb <sup>2+</sup>	Cd <sup>2+</sup>	Pb <sup>2+</sup>
Sample A	100	50	94±3	48±1	98.8±1	49.5±1
Sample B	75	50	65±3	48±1	74±1	49.0±1

\* Bi-HA CME analysis consists of mean for 7 replicates with standard errors

Bi-HA CME offers a well-defined stripping peak with favorable signal-to-background characteristics, and shows no effect from oxygen interference. Apart from Cd<sup>2+</sup> and Pb<sup>2+</sup> interaction with HA sorption as well as complex formation with Bi(II) in 0.1M acetate buffer, higher electrocatalytic activity of Cd<sup>2+</sup> and Pb<sup>2+</sup> may be influenced by factors such as having no trace metals in the structure that can cause disturbance and noise, carbonate ion substitution, and the amorphous and internal porosity characteristic of the electrode designed. This has resulted in effective chelation of metal ions with enhanced coordination leading to higher sensitivity for lower detection limits.

#### 4. CONCLUSIONS

Bismuth-modified electrode is a promising alternative to mercury electrode due to its lower toxicity. HA-CME coupled with deposited bismuth film showed better peaks corresponding to Cd<sup>2+</sup> and Pb<sup>2+</sup> concentration in aqueous media due to the HA sorption properties and complexation capabilities of Bi. The influence of CV and SWV parameters, deposition time and potential, bismuth



concentration and preconcentration time investigated suggest that bismuth and HA possess combinations of many good features for variations of carbon electrodes in Cd<sup>2+</sup> and Pb<sup>2+</sup> analysis.

#### ACKNOWLEDGMENTS

This work was supported by Biomedical Technology MOR under Bioengineering Research group in Universiti Teknologi PETRONAS. Scholarship to Aamir Amanat Ali Khan is acknowledged.

#### References

1. B.E. Reed, S. Arunachalam, B. Thomas, *Environ. Prog.*, 13 (1994):60-64.
2. G. Hanrahan, D.G. Patil, J. Wang, *J. Environ. Monit.*, 6 (2004):657-664.
3. R. Gunigollahalli Kempegowda, P. Malingappa, *Anal. Chim. Acta*, 728 (2012):9-17.
4. V. Mirceski, S.B. Hocevar, B. Ogorevc, R. Gulaboski, I. Drangov, *Anal. Chem.*, 84 (2012):4429-4436.
5. J.C. Quintana, F. Arduini, A. Amine, F. Punzo, G.L. Destri, C. Bianchini, D. Zane, A. Curulli, G. Palleschi, D. Moscone, *Anal. Chim. Acta*, 707 (2011):171-177.
6. S. Anastasova, A. Radu, G. Matzeu, C. Zuliani, U. Mattinen, J. Bobacka, D. Diamond, *Electrochim. Acta*, 73 (2012):93-97.
7. W.J. Yi, Y. Li, G. Ran, H.Q. Luo, N.B. Li, *Sensor Actuat. B-Chem.*, (2012).
8. J. Wang, *Electroanalysis*, 17 (2005):1341-1346.
9. J. Wang, J. Lu, S.B. Hocevar, P.A.M. Farias, B. Ogorevc, *Anal. Chem.*, 72 (2000):3218-3222.
10. Z.D. Anastasiadou, I. Sipaki, P.D. Jannakoudakis, S.T. Girousi, *Anal. Lett.*, 44 (2011):761-777.
11. S. Taufik, N.A. Yusof, T.W. Tee, I. Ramli, *Int. J. Electrochem. Sci.*, 6 (2011):1880-1891.
12. L.S. Rocha, E. Pereira, A.C. Duarte, J.P. Pinheiro, *Electroanalysis*, 23 (2011):1891-1900.
13. D. Pan, L. Zhang, J. Zhuang, T. Yin, W. Lu, W. Qin, *Int. J. Electrochem. Sci.*, 6 (2011):2710-2717.
14. H. Li, J. Li, Z. Yang, Q. Xu, C. Hou, J. Peng, X. Hu, *J. Hazard. Mater.*, 191 (2011):26-31.
15. C. Kokkinos, A. Economou, *Talanta*, 84 (2011):696-701.
16. M.A. El Mhammedi, M. Achak, M. Bakasse, A. Chtaini, *Appl. Surf. Sci.*, 253 (2007):5925-5930.
17. S. Joschek, B. Nies, R. Krotz, A. Gopferich, *Biomaterials*, 21 (2000):1645-1658.
18. E. Landi, A. Tampieri, G. Celotti, R. Langenati, M. Sandri, S. Sprio, *Biomaterials*, 26 (2005):2835-2845.
19. A. Corami, S. Mignardi, V. Ferrini, *J. Colloid Interface Sci.*, 317 (2008):402-408.
20. S. Meski, S. Ziani, H. Khireddine, *J. Chem. Eng. Data*, 55 (2010):3923-3928.
21. S. Meski, S. Ziani, H. Khireddine, S. Boudboub, S. Zaidi, *J. Hazard. Mater.*, 186 (2011):1007-1017.
22. F. Fernane, M.O. Mecherri, P. Sharrock, M. Hadioui, H. Lounici, M. Fedoroff, *Mater. Charact.*, 59 (2008):554-559.
23. J. Li, D. Kuang, Y. Feng, F. Zhang, M. Liu, *Microchim. Acta*, 176 (2012):73-80.
24. Y. Zhang, Y. Liu, X. Ji, C.E. Banks, W. Zhang, *J. Mater. Chem.*, 21 (2011):7552-7554.
25. G. Yang, Y. Wang, F. Qi, *Microchim. Acta*, 177 (2012):365-372